Journal Pre-proofs

Towards the prediction of barrel fill level in twin-screw wet granulation

Sebastian Pohl, Katrina Frey, Peter Kleinebudde

PII:	S0939-6411(24)00254-6
DOI:	https://doi.org/10.1016/j.ejpb.2024.114428
Reference:	EJPB 114428

To appear in: *European Journal of Pharmaceutics and Biopharmaceutics*

Received Date:	6 March 2024
Revised Date:	2 July 2024
Accepted Date:	26 July 2024

Please cite this article as: S. Pohl, K. Frey, P. Kleinebudde, Towards the prediction of barrel fill level in twin-screw wet granulation, *European Journal of Pharmaceutics and Biopharmaceutics* (2024), doi: https://doi.org/10.1016/j.ejpb.2024.114428

This is a PDF file of an article that has undergone enhancements after acceptance, such as the addition of a cover page and metadata, and formatting for readability, but it is not yet the definitive version of record. This version will undergo additional copyediting, typesetting and review before it is published in its final form, but we are providing this version to give early visibility of the article. Please note that, during the production process, errors may be discovered which could affect the content, and all legal disclaimers that apply to the journal pertain.

© 2024 The Author(s). Published by Elsevier B.V.

Journal Pre-proofs

Towards the prediction of barrel fill level in twin-screw wet granulation

Sebastian Pohl[a,b], Katrina Frey[a], Peter Kleinebudde[a,*]

[a] Institute of Pharmaceutics and Biopharmaceutics

Heinrich Heine University

Universitätsstrasse 1, Building 26.22

40225 Düsseldorf, Germany

[b] INVITE GmbH

Drug Delivery Innovation Center

Chempark, Buildung W32

51368 Leverkusen, Germany

E-mail addresses of each author:

Sebastian Pohl sebastian.pohl@hhu.de

Katrina Frey katrina.frey@hhu.de

Peter Kleinebudde kleinebudde@hhu.de

*corresponding author:

phone: +49211 81 14220

E-mail: kleinebudde@hhu.de

Journal Pre-proofs

Journal Pre-proofs

Abstract

The barrel fill level is defined as the fraction of the free available volume for a given screw configuration that is occupied by the wet material and is an interplay of the material throughput, screw speed, screw setup, barrel length of the twin-screw granulator used and the properties of the starting material. The fill level has a major impact on mixing and densification of the wetted mass and thus on the granules produced. It influences the twin-screw granulation process accordingly.

In the current study, a model has been developed which is predictive in terms of material hold-ups in the barrel at various process settings by considering the geometries of the different screw elements in a configuration and the conveying velocity of the wet mass through the barrel. The model was checked on two granulators of different dimensions with various screw configurations, different materials and at different process settings.

The model represents a step forward in predicting the barrel fill level but further research with a broader spectrum of materials, screw configurations and process settings is still needed and additional twin-screw granulators of other dimensions must be investigated.

Keywords

wet granulation, twin-screw granulation, barrel fill level, prediction, predictive model, screw configuration, microcrystalline cellulose, kneading block, stagger angle

Journal Pre-proofs

List of Abbreviations

Symbol	**Abbreviation**
ω	angular velocity
η_v	volumetric efficiency
ρ_{bulk}	bulk density
φ	barrel fill level (dimensionless)
$A_{element}$	free cross-sectional area of screw element
A_m	mean cross-sectional area
CE	conveying element
d_{barrel}	barrel diameter
$d_{element}$	diameter of a screw element
DCPA	dicalcium phosphate anhydrous
f	correction factor
KB	kneading block
KE	kneading element
L/D	length-to-diameter
L/S	liquid-to-solid weight ratio

Journal Pre-proofs

l_{barrel}	barrel length
l_{CE}	length of a conveying element
l_{eff}	effective length
$l_{element}$	length of a screw element
l_{KB}	length of a kneading block
l_{lead}	lead length
l_{rev}	axial length for one screw rotation
l_{screw}	screw length
LPCE	long pitch conveying element
MCC	microcrystalline cellulose
MPCE	medium pitch conveying element
$\dot{m}_{tot}$	total material throughput
$\dot{m}_{p}$	powder feed rate
m_{theo}	theoretical mass hold-up
n	screw speed
N	number of measurements to calculate mean value and standard deviation
t_{mean}	mean residence time

Journal Pre-proofs

t_{turn}	circulation time
PFN	powder feed number
PFR	powder feed rate
PMMA	polymethyl methacrylate
s	standard deviation
SFL	specific feed load
SPCE	short pitch conveying element
TSG	twin-screw granulation
v_a	true velocity
$\overline{v}_{harmonic}$	mean conveying velocity
v_p	net forward velocity
v_t	theoretical velocity
V_{free}	available volume of the entire screw configuration
VSPCE	very short pitch conveying element
w_{crest}	width of the crest of a conveying element
w_{pitch}	width of the pitch of a conveying element
$x_{element}$	number of a specific element used within the screw setup

Journal Pre-proofs

Journal Pre-proofs

1. Introduction

Granulation is a fundamental step in the production of oral solid dosage forms and a widely used technique for size enlargement of powder particles into bigger agglomerates, in which the primary particles still remain distinguishable [1, 2]. Its aim is the improvement of particle and bulk properties, such as the reduction of dust formation, bulk volume, specific surface area and segregation tendency due to the immobilisation of the ingredients in the composition. The lower ratio of adhesion force to weight force improves flow behaviour, die filling during tableting and accuracy in dosing. In case of direct administration, the granules must meet specifications in order to enable packaging, transport and consumer handling. In the likely case of further processing, the porosity of the granules allows for better deformation during tableting and leads to the production of tablets with sufficient mechanical strength [2-6].

In twin-screw wet granulation (TSG), both the powder blend and granulation fluid are fed into the barrel of the granulator. The wetted material is transported from the infeed area towards the barrel exit while experiencing constant agitation exerted by the corotating and intermeshing screws which brings the primary powder particles closer together. The viscous forces, capillary pressure and surface tension of the granulation liquid cause the adhesion of the primary particles to each other and thus granule formation. Subsequent drying leads to the formation of more permanent, solid bonds [2, 7-9].

Several factors are critical for the TSG process and the resulting granules characteristics, such as the screw configuration with, e.g., elements with low or no conveying capacity (kneading blocks at varying offset angles [9-12], distributive feed screws or tooth-mixing elements [12-14]), liquid-to-solid (L/S) ratio and barrel fill level. The barrel fill level is the ratio of the volume that the wet material occupies to the available volume with a certain screw design. When granulating on a twin-screw granulator, the barrel fill level can be directly influenced by adjusting the screw speed and material throughput [9, 15-18]. An increase in material throughput or a reduction in screw speed leads to an increase in barrel fill level. Consequently, the material experiences higher compaction and densification. The granulation liquid is probably better squeezed out of the granule voids by the compaction processes and further distributed by the screws, promoting additional granule growth [19-21]. In contrast, at a starved stage of barrel fill, the wet mass cannot interact sufficiently with each other, potentially leading to particle segregation rather than to an appropriate granule formation and mixing quality. A lack of particle interaction reduces the interparticle friction, leading to less attrition and thus to big granules exiting the barrel [19, 22-24]. Furthermore, the mixing quality also differs at different filling degrees. At low fill levels, axial mixing dominates, while at high filling degrees plug flow prevails. Therefore, the knowledge of the barrel filling degree is particularly crucial for the production of granules, especially when granules with similar characteristics ought to be produced; eventually at different scales or on granulators with different dimensions [19, 25].

A commonly used surrogate is the specific feed load (SFL), a ratio of the gravimetrically fed mass to the screw speed that mirrors the volumetric filling degree by considering the amount of wet mass conveyed per screw turn along the screw axis [15, 26]. It typically has a dimension of a mass and can be calculated according to Eq. (1) [15]

$$SFL = \frac{\dot{m}_{tot}}{n} \quad (1)$$

where $\dot{m}_{tot}$ is the total material throughput and n is the screw speed. Since the SFL is specific to the formulation, the screw configuration and the granulator used, it has only limited validity [15].

Some dimensionless approaches have been proposed to describe the barrel fill level. One of the first of its kind was introduced by Osorio et al. [27] and is shown in Eq. (2)

$$\varphi_{Osorio} = \frac{1}{F_1 \cdot F_2 \cdot F_3} \cdot PFN = \frac{1}{\frac{A_{element}}{d_{barrel}{}^2} \cdot \frac{l_{rev}}{d_{barrel}} \cdot \frac{2\pi \cdot v_p}{\omega \cdot l_{element}}} \cdot \frac{\dot{m}_p}{\rho_{bulk} \cdot \omega \cdot d_{barrel}{}^3} \quad (2)$$

where φ_{Osorio} is the dimensionless barrel fill level, l_{rev} is the length of an element with which the material is pushed forward per screw revolution, $A_{element}$ is the free cross-sectional area of the screw element, v_p is the net forward velocity of the powder, $\dot{m}_p$ is the powder flow rate, ρ_{bulk} is the bulk density of the powder, ω is the angular velocity of the shafts of the screws used to calculate the screw speed by applying $\omega/2\pi$, d_{barrel} is the barrel diameter, F_1-F_3 are dimensionless geometric or velocity ratios and PFN is the dimensionless powder feed number, a ratio of the volumetric flow rate ($\dot{m}_p/\rho_{bulk}$) to the volume turnover at given powder feed rate and screw speed. F_1 is a geometric ratio that refers to the proportion of the barrel's free cross-sectional area after considering the occupied fraction of shaft and screw element, F_2 is a length-to-diameter ratio of a screw element and thus also a geometric ratio, while F_3 is a velocity ratio of the net forward velocity of the powder and the surface velocity of the rotating screw element. F_3 should take into account the fact that the powder moves slower than the screw flight due to slipping of the powder on the element surface, resulting in back-mixing phenomena [27].

The proposal unfortunately has some imprecisions that limits its applicability, e.g. the extent of surface slipping that kept unquantified, resulting in v_p being defined on the basis of estimates and forcing the authors to use only the PFN-part in their study. It was revealed that using PFN for fill level quantification and setting up experiments had no (on x_{10} and x_{50}) or only small effects on granule sizes (x_{90}), whereas the granulator barrel and its dimensions were found to have much greater impact on granule sizes, especially on the development of bigger granules (x_{90}). Besides that, $d_{barrel}{}^3$ seems insufficient to mirror the volume of an entire barrel. Nevertheless, Lute et al. [28], who used the free volume provided by the screw configuration, still showed PFN being similarly less effective as Osorio et al. with regard to x_{50}. Despite varying PFNs, the granule sizes remained almost similar. Thus, the PFN at its current stage might generally be inappropriate for predicting barrel fill level.

Gorringe et al. [29] provided a more practical approach, considering the fraction of the channels of conveying elements filled with powder as ratio of powder flow rate and theoretical maximum screw capacity. The approach is depicted in Eq. (3)

$$\varphi_{Gorringe} = \frac{\dot{m}_p}{\eta_v \cdot \bar{\rho}_{bulk} \cdot V_{free} \cdot \frac{l_{rev}}{l_{screw}} \cdot n} \quad (3)$$

where $\varphi_{Gorringe}$ is the dimensionless barrel fill level, $\dot{m}_p$ is the powder feed rate, η_v is the volumetric efficiency of the screw to convey the material, $\bar{\rho}_{bulk}$ is the mean bulk density of the material in the screw channels, V_{free} is the free volume and l_{screw} is the screw length. The volumetric efficiency is a dimensionless parameter that reflects a ratio between the actual and theoretical volumetric capacity and gives values between 0 and 1 [30].

For $\bar{\rho}_{bulk}$, it was assumed that the liquid is absorbed in the voids of the powder and affects the density value compared to the normal bulk density. The term $V_{free} \cdot \frac{l_{rev}}{l_{screw}}$ reflects the theoretical volume displacement per revolution of the screw. In addition, V_{free} was determined for a screw configuration consisting only of conveying elements, even though other screw setups were used in the studies [16, 18, 29].

Disadvantageous might also be the estimation of η_v which hampers its practical implementation [17], particularly as the decision of when the granulator operates at its maximum capacity is rather subjective.

The similar granule size distributions obtained at similar barrel fill levels (similar φ-values) at different combinations of screw speeds and material throughputs for different screw setups investigated may highlight the suitability of the proposed attempt, but overall, the uncertainty in determining η_v leaves a general vagueness of the approach. However, the extent of uncertainty is likely to be less crucial when all experiments are carried out on the same granulator [16, 18, 29], but has more impact when other granulators with different dimensions are used. So far, the presented approach has not been tested on other granulators.

A similar conclusion has been made by Mundozah et al. [17], who also proposed another approach in which the volumetric flow rate is linked to the volumetric forward conveying rate of the screws. Barrel fill level is then calculated according to Eq. (4)

$$\varphi_{Mundozah} = \frac{v_t}{v_a} = \frac{\frac{\dot{m}}{\rho_{bulk} \cdot A_m}}{\frac{l_{eff}}{t_1}} \qquad (4)$$

where $\varphi_{Mundozah}$ is the dimensionless fill level, v_t is the theoretical velocity, v_a is the true velocity, A_m is the mean cross-sectional area and l_{eff} is the effective length of the screws used. For simplicity, the bulk density was assumed to be constant.

However, the theoretical velocity, v_t, gives the impression that it could reflect a real velocity that can be verified by measurements. Apart from its units, v_t rather reflects a volumetric flow rate, that happens to be related to the mean cross-sectional area and thus leads to a putative velocity. Therefore, v_t is influenced by the screw geometry and the material throughput. The ineffectiveness of v_t is demonstrated by the values given in Table 2-4 in [17], which are constant for certain throughputs and screw setups, even though various different screw speeds were used.

An alleged easy and rather conventional approach is given in Eq. (5), where the mass hold-up, m_{theo}, should be assessable taking into account the total material throughput (in g/s), $\dot{m}_{tot}$, and the mean residence time (in s), t_{mean} [16, 29]

$$m_{theo} = \dot{m}_{tot} \cdot t_{mean} \qquad (5)$$

Although the approach seems convenient, it unfortunately did not work with self-measured residence times and mass hold-ups (data not shown), which is why it can be considered unsuitable.

Having the above mentioned in mind, the (dimensionless) prediction of barrel fill level in TSG can still be regarded as unsolved. This scientific gap is still to be filled with a validated model that takes the real screw configuration and actual process settings into account. It has to be applicable across a wide range of granulators with various dimensions and checked with real measurements. Therefore, the ultimate aim was to develop a new model that meets these requirements and considers both the real conveying velocity of the wet material throughout the barrel at given process conditions as well as particularities in screw configurations that would

Journal Pre-proofs

affect the materials transportation velocity through the barrel and cause increased mass hold-up. Verification should be done at various process settings using different screw setups. The influence of different materials should also be taken into account.

It must be clear that several issues need to be solved first, e.g. density change along the screw axes or the prediction of the amount of wet mass in the barrel at different process settings, in order to create a final model, and that this goal can only be achieved step by step in a longer development process. Thus, we had decided to start with the prediction of mass. At the end of this paper there is a brief discussion on what factors are still missing for a fully predictive model, which may also show the next steps in development.

2. Theoretical Development

2.1 Proposal for the calculation of mass hold-up during TSG

Eq. (6) shows the approach to predict the amount of mass inside the granulator barrel

$$m_{theo} = \frac{l_{barrel}}{\bar{v}_{harmonic}} \cdot \dot{m}_{tot} \cdot f \quad (6)$$

where m_{theo} is the theoretical mass hold-up (in g), l_{barrel} is the barrel length used (in mm), $\bar{v}_{harmonic}$ is the mean conveying velocity of the material through the barrel (in mm/s), $\dot{m}_{tot}$ is the total material throughput (in g/s) and f is a correction factor that covers factors with influence on the amount of mass inside, e.g. friction forces, back-mixing or densification processes in some parts of the screw, that cannot be determined numerically and thus have not yet been listed as individual variables in the given equation. It can be guessed that these factors might influence the amount of mass to different extent, depending on the material properties or the chosen screw setups and process settings.

2.2 Mean conveying distance per revolution

The distance covered axially per revolution by the conveyed material, l_{rev}, seemed to be the right variable for determining the barrel filling degree. It must be taken into account that all elements incorporated in a screw setup have strong influence on l_{rev}, as they possess different conveying capacities [9, 10, 19, 31].

For conveying elements (CEs), which lengths are longer than l_{rev}, l_{rev} was calculated as shown in Eq. (7)

$$l_{rev_{CE}} = 2 \cdot (w_{crest} + w_{pitch}) \quad (7)$$

where w_{crest} is the crest width of a CE and w_{pitch} is width of the element pitch. If the CE has the same length as l_{rev}, like the one exemplarily depicted in Figure 1 (left photograph), the element length, $l_{element}$, was considered equal to l_{rev}. Some element-relevant variables needed for the calculation are given in Figure 1.

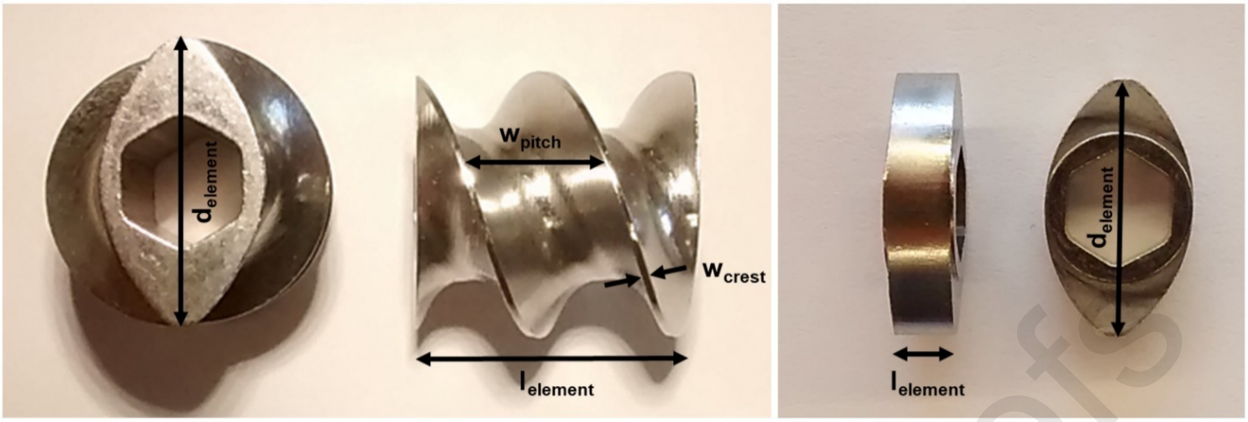

Figure 1. Relevant variables of conveying elements (left) and kneading elements (right). Exemplary photographs of screw elements of the Pharma 16 twin-screw granulator used in the study.

2.3 Mean conveying velocity through the barrel

The mean velocity, $\bar{v}_{harmonic}$, of the material conveyed through the barrel was assessed using Eq. (8)

$$\bar{v}_{harmonic} = \frac{l_{CEX} + l_{CEY} + l_{CE_Z} + l_{KB_X} + l_{KB_Y} + l_{KB_Z}}{\left(\frac{l_{CEX}}{v_{CEX}}\right) + \left(\frac{l_{CEY}}{v_{CEY}}\right) + \left(\frac{l_{CE_Z}}{v_{CE_Z}}\right) + \left(\frac{l_{KB_X}}{v_{KB_X}}\right) + \left(\frac{l_{KB_Y}}{v_{KB_Y}}\right) + \left(\frac{l_{KB_Z}}{v_{KB_Z}}\right)} \quad (8)$$

where the variables l and v are the length of each conveying or kneading block section and the velocities at which the material is transported through these sections. The length (in mm) of a specific type of CE, l_{CE}, or the lengths of differently designed kneading blocks (KB), l_{KB}, due to different arrangements of kneading elements (Figure 1, right photograph), used in the screw configuration, where *X, Y, Z* represent these different types, was calculated according to Eq. (9)

$$l_{CE} = l_{KB} = l_{element} \cdot x_{element} \quad (9)$$

where $x_{element}$ is the number of that specific element used in the screw design.

The conveying velocities (in mm/s) of the material through the conveying and KB sections, v_{CE} and v_{KB}, were calculated by applying Eqs. (10) and (11)

$$v_{CE} = \frac{l_{rev_{CE}}}{\left(\frac{1}{n}\right)} = \frac{l_{rev_{CE}}}{t_{turn}} \quad (10)$$

$$v_{KB} = \frac{l_{KB}}{\left(\frac{x_{element}}{\left(\frac{360}{\sphericalangle}\right)} \cdot \left(\frac{1}{n}\right)\right)} = \frac{l_{KB}}{k \cdot t_{turn}} \quad (11)$$

where n is the screw speed (in s^{-1}), t_{turn} is the circulation time (in s), ($360/\sphericalangle$) is the number of kneading elements (KEs) that would be needed for a complete revolution for a given stagger angle, $x_{element}/(360/\sphericalangle)$ gives the correction factor, k, for t_{turn} when the KB length is unequal to one turn. In case of equality, k will have the value of 1.

3. Materials and Methods

3.1 Materials

Materials used in the study were microcrystalline cellulose (MCC) (Vivapur® 102, JRS Pharma, Rosenberg, Germany), dicalcium phosphate anhydrous (DCPA) (DI-CAFOS® A12, Chemische Fabrik Budenheim, Budenheim, Germany) and lactose monohydrate (FlowLac®100, Meggle, Wasserburg am Inn, Germany). Demineralised water was used as granulation liquid.

3.2 Methods

3.2.1 Preparation of powder blends

The components were given into a lab-scale blender (LM 40, L.B. Bohle, Ennigerloh, Germany) and blended for 20 min at 25 min^{-1}. Two compositions containing MCC and DCPA of varying proportions (20:80 and 60:40 % w/w) were accordingly prepared for the investigation. Also, pure MCC and lactose monohydrate were used in the studies.

3.2.2 Twin-screw granulation

Experiments were carried out on two twin-screw granulators of different dimensions.

Validation initially occurred on a Pharma 16 twin-screw granulator (Thermo Fisher Scientific, Waltham, Massachusetts, USA) using the entire barrel length of 640 mm (barrel L/D 40:1, 1 D is equal to 16 mm as it reflects the barrel diameter). For the calculation according to Eq. (6), a barrel length of 610 mm was used as the first screw element was located in front of the infeed zone and thus did not contribute to mass conveyance. A loss-in-weight feeder (K-SFS-24, K-Tron, Coperion, Niederlenz, Switzerland) was used to feed the blends directly into the barrel. Demineralised water was fed through a nozzle (inner diameter of 0.75 mm) using a micro annular gear pump (MZR 7205, HNP-Mikrosysteme, Schwerin, Germany). Three screw configurations were tested, considering long-pitch conveying elements (LPCE), short-pitch conveying elements (SPCE) and KEs. The first one (hereinafter denoted as setup I) contained only CEs, the second and third configuration

Journal Pre-proofs

contained a KB at 30° (setup II) or 60° (setup III) offset angle. The specific screw designs are given in Table 1. Screw shafts used exceeded the barrel and had a L/D of 41:1 to avoid unintended mass hold-ups at the barrel exit that could have impaired model validation. The powder was fed at the LPCE part while the liquid was infed at the SPCE section downstream the LPCEs. The liquid infeed was set by using the software Motion Manager 4 (Dr. Fritz Faulhaber, Schönaich, Germany) and monitored by a Coriolis mass flow meter (Proline Promass 80A, Endress+Hauser, Reinach, Switzerland). Three powder feed rates (PFR) (1.5, 3.0 and 4.5 kg/h) were investigated at three screw speeds (150, 300 and 450 min^{-1} for 1.5 kg/h and 3.0 kg/h as well as 200, 300 and 450 min^{-1} for 4.5 kg/h) with each screw configuration. Mass hold-ups were determined at steady state conditions.

Verification of the model's predictive accuracy occurred on a Leistritz Micro 27 GL-28D twin-screw granulator (Leistritz Extrusionstechnik, Nürnberg, Germany). Due to a 54 mm-extension, the barrel length was 810 mm (L/D 30:1) and the screw shafts used did not exceed the barrel. However, a barrel length of 785 mm was used for the calculations. The powder blend was fed by a gravimetric loss-in-weight feeder (K-CL-KT 20, K-Tron, Coperion, Niederlenz, Switzerland). Demineralised water was pumped by a peristaltic pump (ecoline VC-MS/CA8-6, Ismatec, Opfikon, Switzerland) into the intermeshing zone between the screws upstream the first kneading zone.

Similar screw configurations as used on Pharma 16 were tested, considering LPCE, medium-pitch CE (MPCE), SPCE, CEs with very small pitches (VSPCE) and ready-to-use KBs. The first and second screw setup (hereinafter denoted as setup A and B, respectively) contained only CEs, with setup B having CEs with narrower pitches incorporated than A, while the third and fourth configuration contained two KBs of five KEs each at 30° (setup C) or 60° (setup D) offset angle (Table 1). Despite similar pitches, the length of the elements used varied, which is why the number given after the CE reflects the element length (in mm). Both the infeed of the powder blend and granulation liquid took place at the initial section of the LPCE part and one after the other. Three PFRs (1.5, 4.5 and 9.0 kg/h) were examined at four screw speeds each. Each PFR was tested at 150, 300 and 400 min^{-1}, while only the lowest screw speed varied depending on the PFR (lowest possible screw speed at 1.5 / 4.5 / 9.0 kg/h: screw setup A and B: 20 / 60 / 120 min^{-1}; setup C and D: 30 / 70 (for 20 % MCC) or 80 (for 100 % MCC) / 130 min^{-1}). Similarly to model validation, mass hold-ups were determined after reaching steady state.

Additional verification experiments occurred on the Pharma 16 twin-screw granulator using lactose monohydrate and a wide range of screw designs containing different numbers of KEs at 30° and 60° stagger angle, set to different numbers of KBs within the design (setup IV-XIII, Table 1). Experiments were carried out at 150, 300 and 450 min^{-1} screw speed in each case and at three PFRs adapted to the screw setup: IV, V and VI at 1.5, 2.25 and 3.0 kg/h, VII and VIII at 1.5, 1.75 and 2.0 kg/h, IX and X at 1.5, 3.0 and 4.5 kg/h, XI and XII at 1.5, 2.25 and 3.0 kg/h, XIII at 1.5, 1.75 and 2.0 kg/h.

All experiments were carried out when the process had reached its steady state, at 25 °C barrel temperature and at 15 % L/S for MCC and MCC-DCPA mixtures, whereas L/S of 7 % was used for lactose monohydrate.

Table 1. Screw setups used in the verification and validation experiments.

Granulator	**Screw setup**	**Detailed configuration**
Pharma 16	I	2x 2D LPCE – 36.5x 1D SPCE

	II	2x 2D LPCE - 10x 1D SPCE - 9x 0.25D KE 30° - 24x 1D SPCE
	III	2x 2D LPCE - 10x 1D SPCE - 9x 0.25D KE 60° - 24x 1D SPCE
	IV	2x 2D LPCE – 10x 1D SPCE – 5x 0.25D KE 30° – 25x 1D SPCE
	V	2x 2D LPCE – 10x 1D SPCE – 9x 0.25D KE 30° – 24x 1D SPCE
	VI	2x 2D LPCE – 10x 1D SPCE – 5x 0.25D KE 30° – 1x 1D SPCE – 5x 0.25D KE 30° – 23x 1D SPCE
	VII	2x 2D LPCE – 10x 1D SPCE – 13x 0.25D KE 30° – 23x 1D SPCE
	VIII	2x 2D LPCE – 10x 1D SPCE – 5x 0.25D KE 30° – 1x 1D SPCE – 5x 0.25D KE 30° – 1x 1D SPCE – 3x 0.25D KE 30° – 21x 1D SPCE
	IX	2x 2D LPCE – 11x 1D SPCE – 5x 0.25D KE 60° – 24x 1D SPCE
	X	2x 2D LPCE – 11x 1D SPCE – 5x 0.25D KE 60° – 2x 1D SPCE – 5x 0.25D KE 60° – 21x 1D SPCE
	XI	2x 2D LPCE – 11x 1D SPCE – 10x 0.25D KE 60° 23x 1D SPCE
	XII	2x 2D LPCE – 10x 1D SPCE – 5x 0.25D KE 60° – 1x 1D SPCE – 5x 0.25D KE 60° – 1x 1D SPCE – 4x 0.25D KE 60° – 21x 1D SPCE
	XIII	2x 2D LPCE – 10x 1D SPCE – 14x 0.25D KE 60° – 23x 1D SPCE
Leistritz Micro 27 GL-28D	A	7x LPCE90 - 1x MPCE90 - 1x SPCE90
	B	3x LPCE90 - 2x SPCE90 - 2x MPCE90 - 1x VSPCE60 - 1x VSPCE30 - 1x SPCE90
	C	5x LPCE90 – 1x KB 30° - 1x MPCE30 – 1x KB 30° - 1x MPCE90 – 1x LPCE90 + 1 SPCE90

	D	5x LPCE90 – 1x KB 60° - 1x MPCE30 – 1x KB 60° - 1x MPCE90 – 1x LPCE90 + 1 SPCE90

3.2.3 Measurement of screw elements

In order to determine the variables needed for the calculation in the current study, the screw elements were measured with regard to their dimensions using a calliper (Garant digital DC2, Hoffmann Group, München, Germany).

3.2.4 Determination of mass hold-up during TSG

The process (screws, powder feeder, liquid pump) was stopped and both the barrel outlet and the screw part exceeding the barrel (valid for Pharma 16 granulator) were cleaned from unwanted material remains. Afterwards, the screws were started and the material exiting the barrel was collected and weighed on a precision balance (1507 004, Sartorius, Göttingen, Germany). This procedure was performed five times for each setting.

3.2.5 Determination of factor *f* using non-linear curve fit

Factor f was determined by applying the non-linear fit application (NLFit) of the OriginPro 2021 software by implementing Eq. (6) as predictive model in the software with $\bar{v}_{harmonic}$ as independent and m_{theo} as dependent variables. Factor f was then determined by assigning numerical values to the independent variable and the other variables, except for f, at first and using the Levenberg-Marquardt algorithm for iteration afterwards. Thus, the adaption of the predictions to the measured ones occurred only on the basis of changing f. Determination occurred for each screw configuration, formulation and material throughput.

4. Results and discussion

4.1 Measurements of screw elements

An overview of the measurements of the screw elements can be found in Table 2. The smaller w_{pitch}, the shorter the distance covered per screw turn. This means that more revolutions are required to transport the material through the barrel. However, the element length of the 1D-SPCE of the Pharma 16 granulator covers an entire helix turn, which is why it was not necessary to measure w_{crest} and w_{pitch} as $l_{element}$ is equal to l_{rev} (see section 2.2). The same applies to the 0.5D-SPCE as it is basically half a 1D element.

Table 2. Information on screw elements of the different twin-screw granulators (N=6, mean values).

Granulator	Variable	$l_{element}$	l_{KB}	$d_{element}$	w_{pitch}	w_{crest}

	Unit	mm	mm	mm	mm	mm
Pharma 16	LPCE	31.98	-	15.53	10.14	0.98
	SPCE 1D	15.99	-	15.52	-[a]	-[a]
	SPCE 0.5D	8.00	-	15.49	-[b]	-[b]
	KE	3.99	-	15.55	-	-
Leistritz Micro 27 GL-28D	LPCE90	90	-	26.79	16.74	2.33
	MPCE30	29.99	-	26.79	12.98	1.54
	MPCE90	90	-	26.78	12.94	1.6
	SPCE90	89.99	-	26.85	8.53	1.28
	VSPCE30	30.01	-	26.81	6.32	0.84
	VSPCE60	60.01	-	26.89	6.31	1.18
	KB 30°	-	29.98	26.81	-	-
	KB 60°	-	29.99	26.87	-	-

[a]1D: one helix turn covers $l_{element}$, [b]0.5 D: half helix turn covers $l_{element}$

Journal Pre-proofs

4.2 Model validation

In Figure 2, the results of the validation part can be found, while the determined values of factor *f* are given in Table 3.

As can be seen from Table 3, the influences currently covered by *f* seem to contribute to mass hold-up to different extents, as different *f*-values were determined, despite the same process conditions (PFR, screw speed) being investigated. It might be assumed that friction forces (between the particles and between the wet material and the surfaces of the inner barrel wall and screw elements) were primarily responsible for the increased mass hold-up in screw design types such as setup I, while the mass hold-up obtained in screw setup II and III might rather be attributed to the offset angles and their flow-inhibiting properties, which caused the material to be compacted both upstream and in the KB sections and thus to accumulate [10]. It is also evident from Table 3 that the formulation considerably influences the outcome. Nevertheless, many other influences could also contribute to the results. The results, however, definitely show the necessity of a differentiated view when predicting mass hold-ups for different screw complexities and formulations. Without *f*, predictions would underestimate the mass hold-ups in any case, independently of the screw setup and formulations. As depicted, the *f* values for formulations containing 20 and 60 % MCC were similar amid a given screw setup, whereas essentially higher values were determined for pure MCC, which was assumed to be a consequence of a potential swelling effect of MCC. Due to averaging, the factor values have to be understood as compromise for a certain screw setup, various formulations as well as process settings when using them for predictions.

Using the averaged *f* revealed a good fit between mass predictions and measurements (Figure 2); *f* of 1.40 for screw setup I basically resulted in good matches for all formulations, indicating a solid predictive power for this type of screw configuration. Due to the mentioned compromise, slight deviations could be observed for predictions at 3 and 4.5 kg/h PFR at low screw speeds for pure MCC, but the potential effect on granule characteristics might be marginal in this case as there are no flow obstacles within the screw setup that might alter granule characteristics.

Similarly was observed for screw setups II and III when using *f* of 1.70 and 1.85, respectively. Since predictive errors seemed highest for pure MCC at higher material throughputs and low screw speed among all screw setups, swelling effects of MCC might have increased the volume and thus basically the need for more space. However, owing to the confined space provided by the inner barrel wall and screw elements, the volume increase might have led to higher friction (interparticle, between inner barrel surfaces and the wet mass). It can be assumed that the material was hampered in its flow, causing more back-mixing and resulting in higher mass hold-up (Figure 2G, H and I). In contrast, swelling seemed less prevailing at higher screw speeds as predictive errors were low.

However, the understanding of the mechanisms taking place inside the barrel are generally limited by now, particularly density changes along the screw from powder and liquid infeed towards the barrel exit. Further testing is, therefore, strongly needed.

Journal Pre-proofs

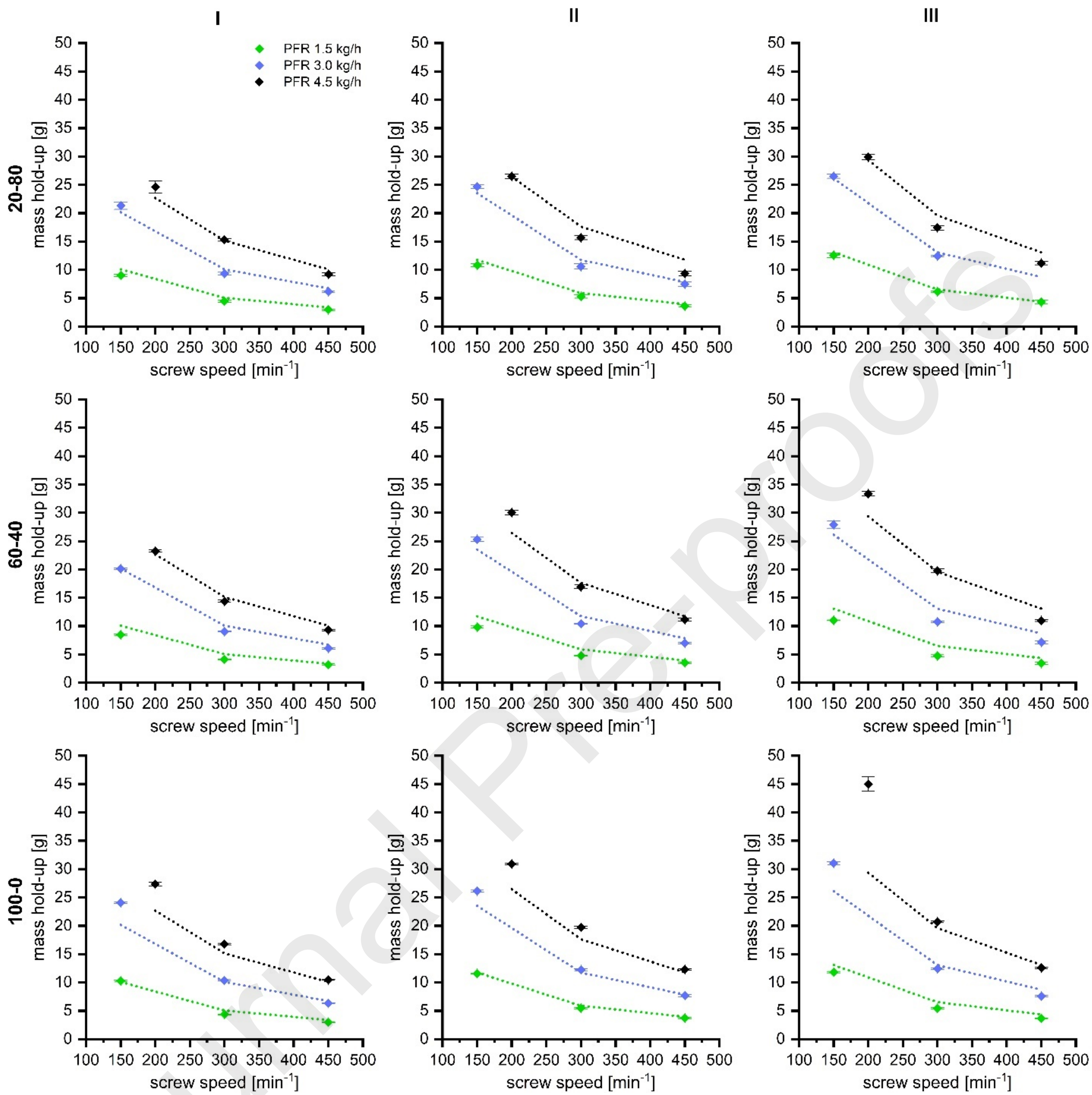

Figure 2. Predicted vs. measured mass hold-ups for various screw speeds and mass throughputs investigated with the different formulations of MCC-DCPA (% m/m) and screw setups (N=5, mean ± s).

Journal Pre-proofs

Table 3. Results for *f* determined with non-linear curve fit for the different formulations and screw setups (*N=3 due to three investigated material throughputs, **N=9, mean ± s).

Screw setup	Formulation MCC:DCPA [% w/w]	*f** [-]	Averaged *f*** [-]
I	20:80	1.38 ± 0.12	1.40 ± 0.14
	60:40	1.31 ± 0.11	
	100:0	1.53 ± 0.14	
II	20:80	1. 63 ± 0.08	1.70 ± 0.16
	60:40	1.66 ± 0.21	
	100:0	1.81 ± 0.15	
III	20:80	1.71 ± 0.04	1.85 ± 0.29
	60:40	1.78 ± 0.24	
	100:0	2.05 ± 0.41	

4.3 Model validation using literature data

To extend the validity, additional literature was identified in which all information necessary (e.g. screw setups, process settings, mass hold-ups in the barrel) was provided [17, 29]. Gorringe et al. [29], unfortunately, did not reveal if the entire barrel length was used or at which position the infeed of the powder blend occurred. In order to avoid speculations, the publication could not be considered. Luckily, screw setups A and C of Mundozah et al. [17] were entirely comparable to the setups I and III used in the investigation above. Screw setup B was indeed different from the screw setups used in our study and therefore also not considered. The determined *f* values considered for validation are given in Table 4.

In addition to the findings made in our study, the analysis of the literature data again highlights that a general factor for predicting mass hold-ups, universally valid for different screw types, is unattainable as the screw setup considerably influences both the conveying velocity and the barrel fill level [9, 10, 19].

Even though the values of *f* for screw setup C of Mundozah et al. (only CEs) are based on the investigation of one material throughput only, the numerical values reveal to be the lowest (1.26 and 1.43), indicating material properties and process settings having minor effects on *f* for this type of configuration. These results are similar to our study. However, the impact on *f* changes with increasing screw complexity. The materials seem likely to influence *f*. The higher variability observed with PMMA and setup A is a consequence of the higher value obtained for PFR 1 kg/h that distorts the averaged *f* value. A similarly high *f* has been determined for lactose monohydrate and screw setup A. As only one PFR had been investigated it can only be guessed that factors of other PFRs would also be lower as observed for PMMA, but the results shown in Table 3 and Table 4 clearly emphasize the influence of the formulation and material throughput on *f*. However, in contrast to screw setups containing only CEs, where *f* has been found similar (1.26 and 1.43), regardless of material properties, the understanding of the actual impacts on *f* is too limited to fully evaluate and assess the results obtained in onefold investigations. Therefore, further tests are necessary to gain more knowledge. Until then, single *f* values obtained with complex screw setups must be excluded from further model setup.

In Figure 3, the averaged *f* values determined for the different formulations are depicted as a function of the number of KEs at 60° offset angle. It is obvious that *f* increases with the incorporation of additional KEs as also more material remains inside the barrel. The correlation coefficient reveals a positive linear relationship (R= 0.9426), which supports the proclaimed dependence. However, the model's applicability is still limited as all investigations, including the literature data, have been performed on the same type of granulator (same barrel diameter, same manufacturer). In addition, based on the number of results available for each figure setup (several for zero and nine KEs, while only one for more KEs), the plot clearly is susceptible to outliers, which might lower the predictive force for screw setups with ten or more KEs. To eliminate this risk, further research, including twin-screw granulators of other dimensions, process settings and other configurations, is needed. Due to the limited number of studies using screw setups with KEs at other offset angles, a correlation plot for 30° offset angle was unfortunately impossible at this stage of research.

To verify the approach, the functional equation in Figure 3 was used to calculate *f* for screw setups with different numbers of KEs at 60° offset angle within the validation window.

Journal Pre-proofs

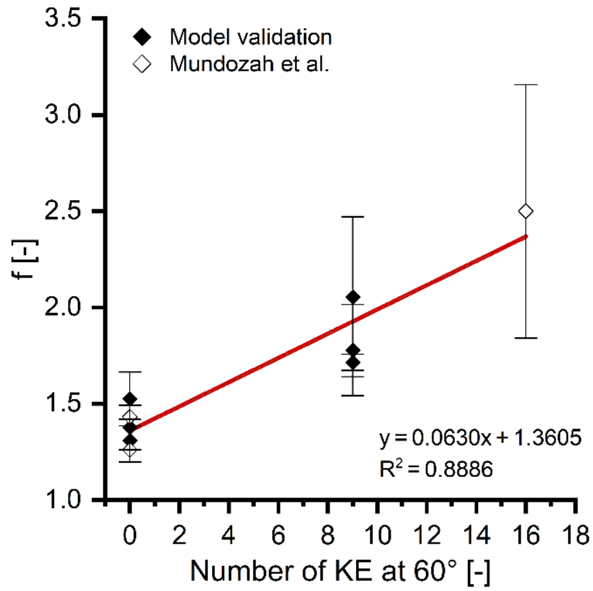

Figure 3. Correlation plot of the averaged *f* values with the number of KEs at 60° stagger angle in the screw setup: 0 (only CE), 9 or 16 (N=1 or N=3, mean ± s).

Journal Pre-proofs

Table 4. Compilation of literature data [17] considered for model validation. Factor *f* determined with non-linear curve fit for the given materials and respective screw configurations (N=1; **N=3, mean ± s).

Material	**Granulator**	**Screw configuration**	**PFR** [kg/h]	**$\dot{m}_{tot}$** [kg/h]	**n** [min^{-1}]	**f*** [-]
Polymethyl methacrylate (PMMA)	16 mm Prism Euro Lab Twin-Screw Granulator (Thermo Fisher)	Screw A: 2x 8x0.25D KE 60°, rest CE (2x2D LPCE, rest SPCE)	1.0	1.10	100-300-500-900	2.50 ± 0.66**
			2.0	2.20	100-300-500-900	
			3.0	3.30	100-300-500-900	
		Screw C: Only CE (2x2D LPCE, rest SPCE)	1.0	1.10	100-300-500-900	1.26
Lactose monohydrate		Screw A: see above	1.0	1.10	100-300-500-900	3.88
		Screw C: see above	1.0	1.10	100-300-500-900	1.43

Journal Pre-proofs

4.4 Model verification

Despite the greater dimension of the Leistritz granulator, predicted and measured mass hold-ups basically correlate well for each setup (Figure 4A-C). The results of both formulations investigated scatter around the ideal line (dashed line). Greater deviations, of approximately 10 %, mainly occur in investigations of formulation containing 20 % MCC (partially filled diamonds) at extremely high barrel fill level at mainly low screw speeds, but predictive errors decrease with increasing screw speed at the same PFR. Contrarily, the likelihood for noticeable deviations seem to increase with increasing PFRs, but, except for screw setup A, no general trend can be identified. Similar conclusions can be drawn for pure MCC (filled diamonds), even though the decrease in the predictive error is less pronounced with increasing screw speeds. Higher scattering for setup D, compared to A, might follow a logical reason due to the additional obstacle provided by the KBs, but further investigation with a broader spectrum of material is necessary to confirm or debunk. Verification experiments on Pharma 16 (Figure 4D-H) show, contrarily, an alleged trend towards more material inside the barrel than predicted; largest predictive errors are obtained at high barrel fill levels, particularly at high mass throughputs, but predictability increases with increasing screw speeds. It can be guessed that the freely soluble behaviour of lactose monohydrate used for the investigation causes the formation of a sticky mass inside the barrel, that together with the high fill levels (material tightly packed) makes transport difficult, especially through the KB section(s), which may have resulted in additional mass hold-up. However, this effect seems to be levelled out with increasing screw complexity (more KEs incorporated) as the predictive error decreases. In addition, data also imply improved replicability with increasing screw complexity as standard deviations considerably decrease, independently of the investigated process parameters.

Nevertheless, as only screw setups with KEs at 60° stagger angle have been investigated, conclusions apply to this kind of screws only. At this stage of the investigation, the model predicts mass hold-ups well at different process settings, but the model must still be further improved. It needs to be emphasized that the predicted values represent only mean values without any variability, whereas the process itself is subject to a certain dynamic. This generally influences interpretation. In order to target a fully comprehensive predictive model, permitted deviation/error from the predicted value needs to be defined in one of the next steps of model development.

Taking into account all results obtained during model validation and verification, it can be said that, despite the deviations observed, the correlation plot (Figure 5) shows a strong linear relationship ($R=0.9775$, $p=1.96\cdot10^{-71}$) between measured and predicted values at defined process conditions. Even though the dimensions of the barrel and screw elements of the Leistritz Micro 27 GL-28D are considerably bigger than for model validation, predictions and measurements reveal good matches. Based on this, the model is found suitable for predicting mass hold-ups, independently of the barrel and screw dimensions.

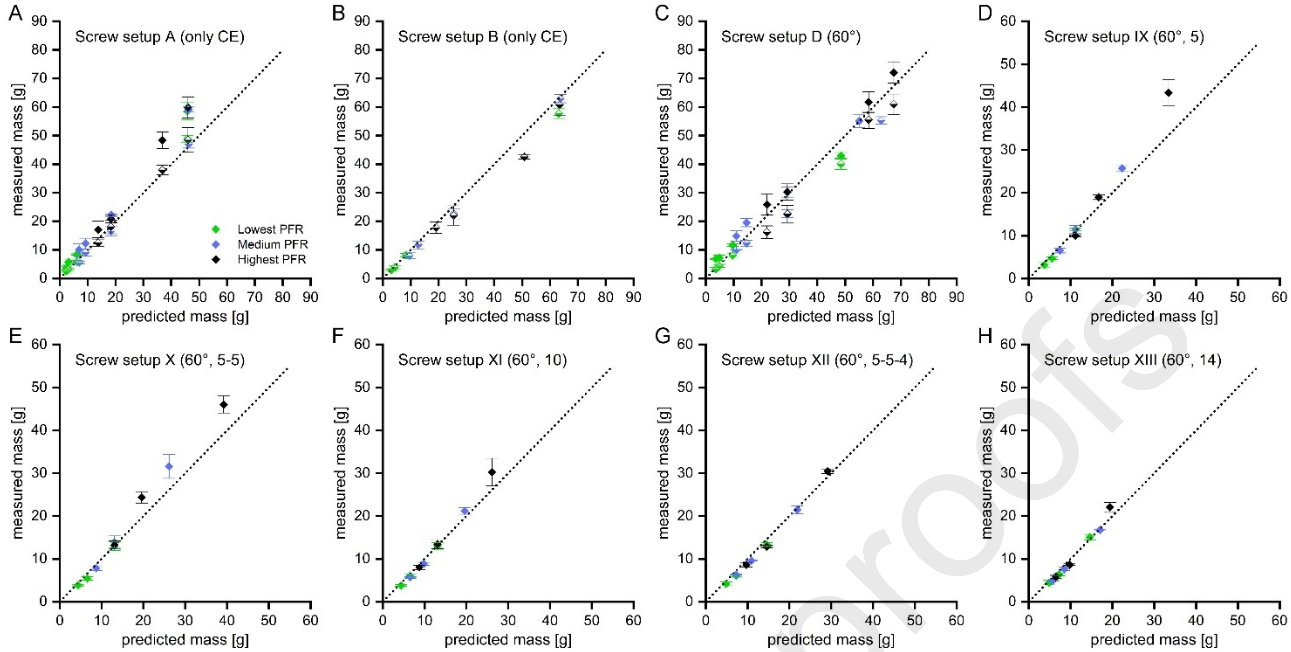

Figure 4. Predicted and measured mass hold-ups of verification experiments: A-C) Leistritz Micro 27 GL-28D and D-H) Pharma 16 (N=3-5, mean ± s). Investigated screw setups are indicated in the top-left corner of each graph, including the main characteristics of the KEs.

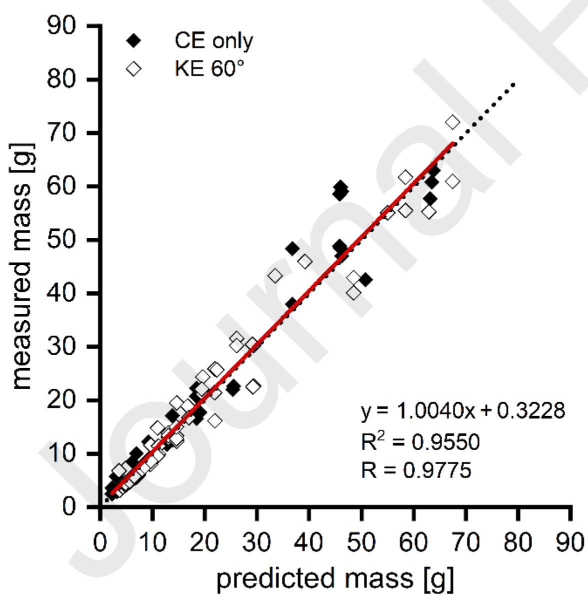

Figure 5. Correlation between predicted and measured mass hold-ups.

Journal Pre-proofs

In addition, the results obtained with the various screw setups at the different process settings were further analysed as described above; by applying non-linear curve fit to determine the respective *f* values. A compilation can be found in Figure 6. Taking into account the different screw diameters of the granulators used, the averaged *f*-values are plotted as a function of the total length of the KEs incorporated in the screw given in number of element diameter, namely $l_{KB}/d_{element}$. Also, as the number of data had been found sufficient, a graph could be plotted for screw setups with KBs of 30° stagger angle (Figure 6A), while the already existing data for 60° offset had been extended with the new results (Figure 6B). The *f* of 2.24 ± 0.28 at 2.2 $l_{KB}/d_{element}$ in Figure 6A originates from the test with 100 % MCC on the Leistritz granulator. So far, there is no adequate explanation as to why this data point deviates so strongly upwards, compared to the other values determined. However, since a deviation to higher *f* (1.74 ± 0.01) can also be observed when using screw setup A (CEs only), this seems to be related to the material used. No such observation can be made for setups with KBs at 60° offset angle. Nevertheless, in both cases, a high positive linear relationship is given, showing that *f* increases with the incorporation of additional KEs in order to also mathematically take into account the additional flow-impeding property [10, 19]. The correlation coefficients are statistically significant (30°: $R=0.7459$, $p=3.8\cdot10^{-4}$, 60°: $R=0.9136$, $p=4.7\cdot10^{-8}$), implying that the latest version of the model is heading in the right direction. Nevertheless, further data points are needed to both strengthen and widen the applicability of the model.

Journal Pre-proofs

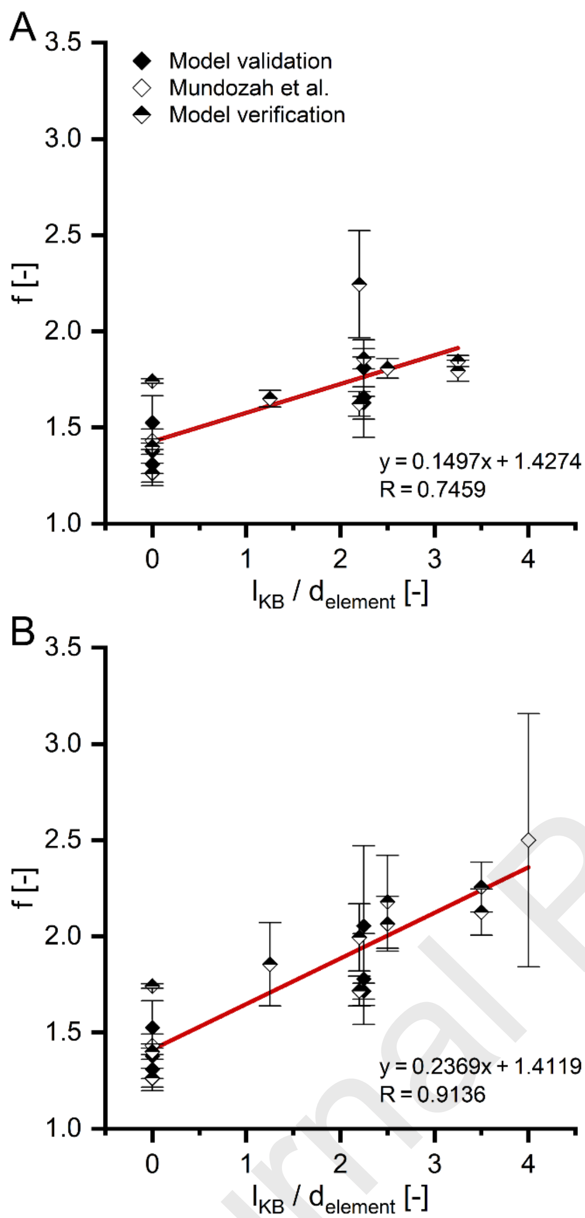

Figure 6. Correlation plot of the averaged *f* values, obtained during all conducted experiments, with the total length of KEs as a number of element diameter, $d_{element}$, for screw designs containing KEs at A) 30° and B) 60° stagger angle (N=1 or N=3, mean ± s).

5. Potential next steps in the development of a fully predictive model

Despite the promising results, the model is still at a development stage, which is why more steps still need to be taken before a fully validated model is available. The inclusion of other important parameters that have not yet been considered as individual ones as well as the definition of acceptable boundaries for variations in prediction could be the next logical steps.

The free available volume, V_{free} (in cm^3), of the screw configuration used and the material density, ρ (in g/cm^3), seem to be such important parameters that are still missing. The volume of the screw configurations (or single elements) can easily be determined by water displacement measurements, while the barrel volume can either be calculated or, if possible, provided by the granulator manufacturer. Definition of material density is even harder as the value may change along the screw length when passing certain sections, e.g. conveying or kneading sections, and thus might be difficult to depict in a single value. From our process understanding, the density might range between the bulk density of the dry formulation (achieved at the powder infeed), and true density of the wet formulation, depending on processes taking place inside the barrel, such as constant densification and loosening in the intermeshing zone due to the supply and removal of material through the front and rear screw, respectively. Next to that, the addition of granulation liquid and with this the wetting properties, the solubility of the individual components of the formulation and the amount of liquid evaporation along the screw, depending on temperature setting, frictional forces (temperature increase), the unused available volume in which the liquid can enter the gas phase and the materials residence time inside the barrel, may affect the density, which is why further investigation is recommended.

All influences on mass hold-up currently covered by the factor f need to be analysed in detail in order to assess the extent of their contribution, and afterwards removed from f and implemented as individual variables. As already mentioned initially, mass hold-up might be affected by friction forces, back-mixing, material properties (swelling, brittle vs. deformable) and densification processes. However, the listing does not claim to be complete.

Furthermore, the model in its current state predicts values that mirror mean values. As the process itself is dynamic and therefore show scattering around the target settings (e.g. powder and liquid infeed), the predictive model should reflect similar dynamics. This will help assessing deviations between real results and predicted values.

Last but not least, the ultimate goal of model development should be the creation of a dimensionless version as it may support upscaling and process transfer activities onto other granulators by keeping the value of the dimensionless term constant. In this regard, dimensional analysis could be a helpful tool [32, 33]. Nevertheless, further investigation is needed to gain much better process understanding as this might be needed first in order to achieve that ultimate goal.

Journal Pre-proofs

6. Conclusion

A new predictive model for the quantification of the mass hold-up within the barrel during TSG processes has been developed, considering the conveying velocity of the wet material throughout the granulator barrel for different screw setups at defined process settings. Thus, the dimensions of the screw elements including their axial conveying capacity were determined. In addition, a mathematical description of the flow-impeding characteristic of kneading blocks and their resulting effect on mass hold-up was incorporated. During model validation, usage of non-linear curve fitting essentially improved the model's predictability with regards to precise predictions of the mass hold-ups.

The model was later checked by several further experiments, amongst others on granulators of different dimensions and with various screw designs. However, the obtained results were still used to further improve the model's predictive strength. The resulting and latest stage of model development shows strong positive linear relationships for mass hold-ups as well as for screw setups containing KEs at 30° and 60° stagger angles, implying an additional value of the model itself in twin-screw granulation. However, further studies with various materials, granulators, screw designs and process settings are still needed to broaden its applicability and, eventually, to make it relevant for the pharmaceutical industry. Nevertheless, the current version of the model can only be seen as a first step; many more steps are still needed until a fully validated model is available. Once this might be achieved, a classification into different barrel filling states, e.g. starved or flooded, should be attempted as the granule properties can be assumed to differ with the prevailing barrel filling condition.

Acknowledgements

The authors gratefully acknowledge Leah Schlüsener and Luna Maschke for their contribution in the study above described by determining some of the mass hold-ups.

The authors also thank the Drug Delivery Innovation Center (DDIC) for providing the scientific platform and financial support for Sebastian Pohl.

Journal Pre-proofs

References

[1] B.J. Ennis, J.D. Litster, T. Allen, R.H. Snow, Size Reduction and Size Enlargement, in: R.H. Perry (Ed.) Perry's Chemical Engineer's Handbook, McGraw-Hill, New York, 1997, pp. 1748-1836.

[2] S.M. Iveson, J.D. Litster, Growth regime map for liquid-bound granules, AIChE Journal, 44 (1998) 1510-1518.

[3] R. Boerefijn, P.-R. Dontula, R. Kohlus, Chapter 14 Detergent granulation, in: A.D. Salman, M.J. Hounslow, J.P.K. Seville (Eds.) Handbook of Powder Technology, Elsevier Science B.V., 2007, pp. 673-703.

[4] G.I. Tardos, M.I. Khan, P.R. Mort, Critical parameters and limiting conditions in binder granulation of fine powders, Powder Technology, 94 (1997) 245-258.

[5] L. Fries, J. Dupas, M. Bellamy-Descamps, J. Osborne, A.D. Salman, S. Palzer, Bonding regime map for roller compaction of amorphous particles, Powder Technology, 341 (2019) 51-58.

[6] G.M. Walker, Chapter 4 Drum Granulation Processes, in: A.D. Salman, M.J. Hounslow, J.P.K. Seville (Eds.) Handbook of Powder Technology, Elsevier Science B.V., 2007, pp. 219-254.

[7] M.R. Thompson, Twin screw granulation – review of current progress, Drug Development and Industrial Pharmacy, 41 (2015) 1223-1231.

[8] C. Köster, S. Pohl, P. Kleinebudde, Evaluation of Binders in Twin-Screw Wet Granulation, Pharmaceutics, 13 (2021) 241.

[9] A. Kumar, M. Alakarjula, V. Vanhoorne, M. Toiviainen, F. De Leersnyder, J. Vercruysse, M. Juuti, J. Ketolainen, C. Vervaet, J.P. Remon, K.V. Gernaey, T. De Beer, I. Nopens, Linking granulation performance with residence time and granulation liquid distributions in twin-screw granulation: An experimental investigation, European Journal of Pharmaceutical Sciences, 90 (2016) 25-37.

[10] K.T. Lee, A. Ingram, N.A. Rowson, Twin screw wet granulation: The study of a continuous twin screw granulator using Positron Emission Particle Tracking (PEPT) technique, European Journal of Pharmaceutics and Biopharmaceutics, 81 (2012) 666-673.

[11] A.S. El Hagrasy, J.D. Litster, Granulation Rate Processes in the Kneading Elements of a Twin Screw Granulator, AIChE Journal, 59 (2013) 4100-4115.

[12] D. Djuric, P. Kleinebudde, Impact of screw elements on continuous granulation with a twin-screw extruder, Journal of Pharmaceutical Sciences, 97 (2008) 4934-4942.

[13] R. Sayin, L. Martinez-Marcos, J.G. Osorio, P. Cruise, I. Jones, G.W. Halbert, D.A. Lamprou, J.D. Litster, Investigation of an 11mm diameter twin screw granulator: Screw element performance and in-line monitoring via image analysis, International Journal of Pharmaceutics, 496 (2015) 24-32.

[14] J. Vercruysse, A. Burggraeve, M. Fonteyne, P. Cappuyns, U. Delaet, I. Van Assche, T. De Beer, J.P. Remon, C. Vervaet, Impact of screw configuration on the particle size distribution of granules produced by twin screw granulation, International Journal of Pharmaceutics, 479 (2015) 171-180.

Journal Pre-proofs

[15] R. Meier, K.-P. Moll, M. Krumme, P. Kleinebudde, Impact of fill-level in twin-screw granulation on critical quality attributes of granules and tablets, European Journal of Pharmaceutics and Biopharmaceutics, 115 (2017) 102-112.

[16] P. Pawar, D. Clancy, L. Gorringe, S. Barlow, A. Hesketh, R. Elkes, Development and Scale-Up of Diversion Strategy for Twin Screw Granulation in Continuous Manufacturing, Journal of Pharmaceutical Sciences, 109 (2020) 3439-3450.

[17] A.L. Mundozah, J. Yang, C. Omar, O. Mahmah, A.D. Salman, Twin screw granulation: A simpler re-derivation of quantifying fill level, International Journal of Pharmaceutics, 591 (2020) 119959.

[18] C. Mendez Torrecillas, L.J. Gorringe, N. Rajoub, J. Robertson, R.G. Elkes, D.A. Lamprou, G.W. Halbert, The impact of channel fill level on internal forces during continuous twin screw wet granulation, International Journal of Pharmaceutics, 558 (2019) 91-100.

[19] A. Kumar, J. Vercruysse, M. Toiviainen, P.-E. Panouillot, M. Juuti, V. Vanhoorne, C. Vervaet, J.P. Remon, K.V. Gernaey, T. De Beer, I. Nopens, Mixing and transport during pharmaceutical twin-screw wet granulation: Experimental analysis via chemical imaging, European Journal of Pharmaceutics and Biopharmaceutics, 87 (2014) 279-289.

[20] D. Djuric, P. Kleinebudde, Continuous granulation with a twin-screw extruder: Impact of material throughput, Pharmaceutical Development and Technology, 15 (2010) 518-525.

[21] R.M. Dhenge, J.J. Cartwright, M.J. Hounslow, A.D. Salman, Twin screw wet granulation: Effects of properties of granulation liquid, Powder Technology, 229 (2012) 126-136.

[22] E.I. Keleb, A. Vermeire, C. Vervaet, J.P. Remon, Twin screw granulation as a simple and efficient tool for continuous wet granulation, International Journal of Pharmaceutics, 273 (2004) 183-194.

[23] R.M. Dhenge, J.J. Cartwright, D.G. Doughty, M.J. Hounslow, A.D. Salman, Twin screw wet granulation: Effect of powder feed rate, Advanced Powder Technology, 22 (2011) 162-166.

[24] R.M. Dhenge, K. Washino, J.J. Cartwright, M.J. Hounslow, A.D. Salman, Twin screw granulation using conveying screws: Effects of viscosity of granulation liquids and flow of powders, Powder Technology, 238 (2013) 77-90.

[25] T.C. Seem, N.A. Rowson, A. Ingram, Z. Huang, S. Yu, M. de Matas, I. Gabbott, G.K. Reynolds, Twin screw granulation — A literature review, Powder Technology, 276 (2015) 89-102.

[26] K. Kolter, M. Karl, A. Gryczke, Hot-Melt Extrusion with BASF Pharma Polymers Extrusion Compendium, 2nd ed., BASF SE, 2012.

[27] J.G. Osorio, R. Sayin, A.V. Kalbag, J.D. Litster, L. Martinez-Marcos, D.A. Lamprou, G.W. Halbert, Scaling of continuous twin screw wet granulation, AIChE Journal, 63 (2017) 921-932.

[28] S.V. Lute, R.M. Dhenge, A.D. Salman, Twin Screw Granulation: An Investigation of the Effect of Barrel Fill Level, Pharmaceutics, 10 (2018) 67.

[29] L.J. Gorringe, G.S. Kee, M.F. Saleh, N.H. Fa, R.G. Elkes, Use of the channel fill level in defining a design space for twin screw wet granulation, International Journal of Pharmaceutics, 519 (2017) 165-177.

[30] A.K. Srivastava, C.E. Goering, R.P. Rohrbach, D.R. Buckmaster, Chapter 14 Conveying of Agricultural Materials, ASABE, St. Joseph, MI, 2006.

[31] A. Gautam, G.S. Choudhury, Screw configuration effects on residence time distribution and mixing in twin-screw extruders during extrusion of rice flour, Journal of Food Process Engineering, 22 (1999) 263-285.

[32] S. Pohl, P. Kleinebudde, A review of regime maps for granulation, International Journal of Pharmaceutics, 587 (2020) 119660.

[33] M. Zlokarnik, Scale-Up in Chemical Engineering, 1st ed., Wiley-VCH Verlag GmbH & Co. KGaA, Weinheim, 2002.

Journal Pre-proofs

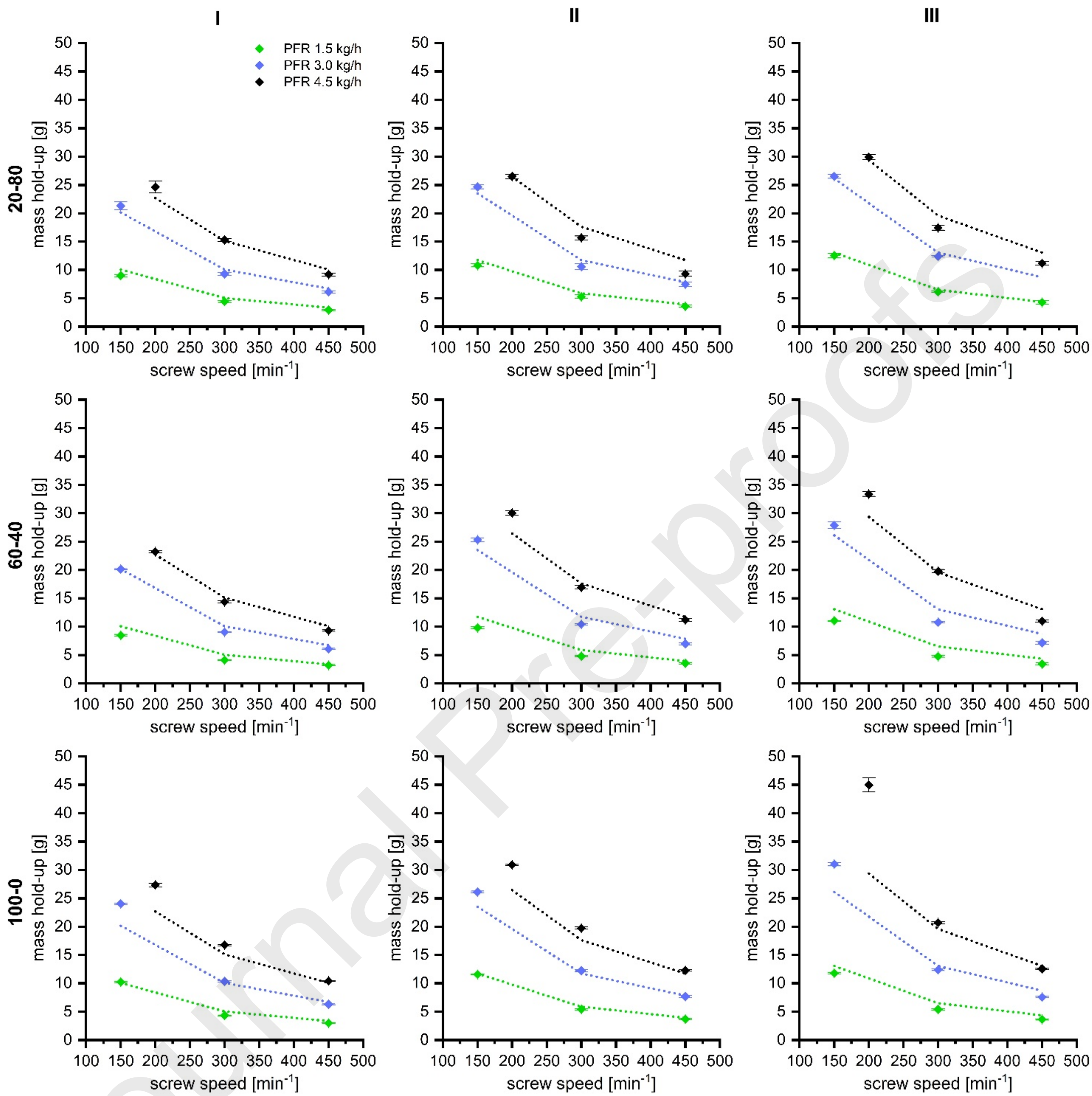

Journal Pre-proofs

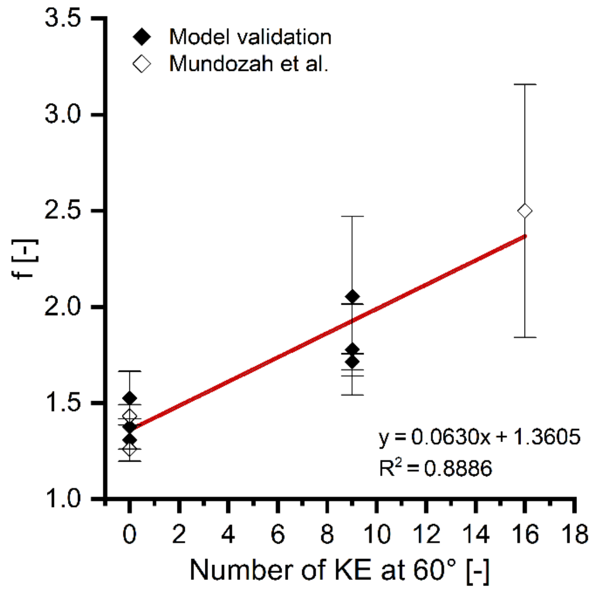

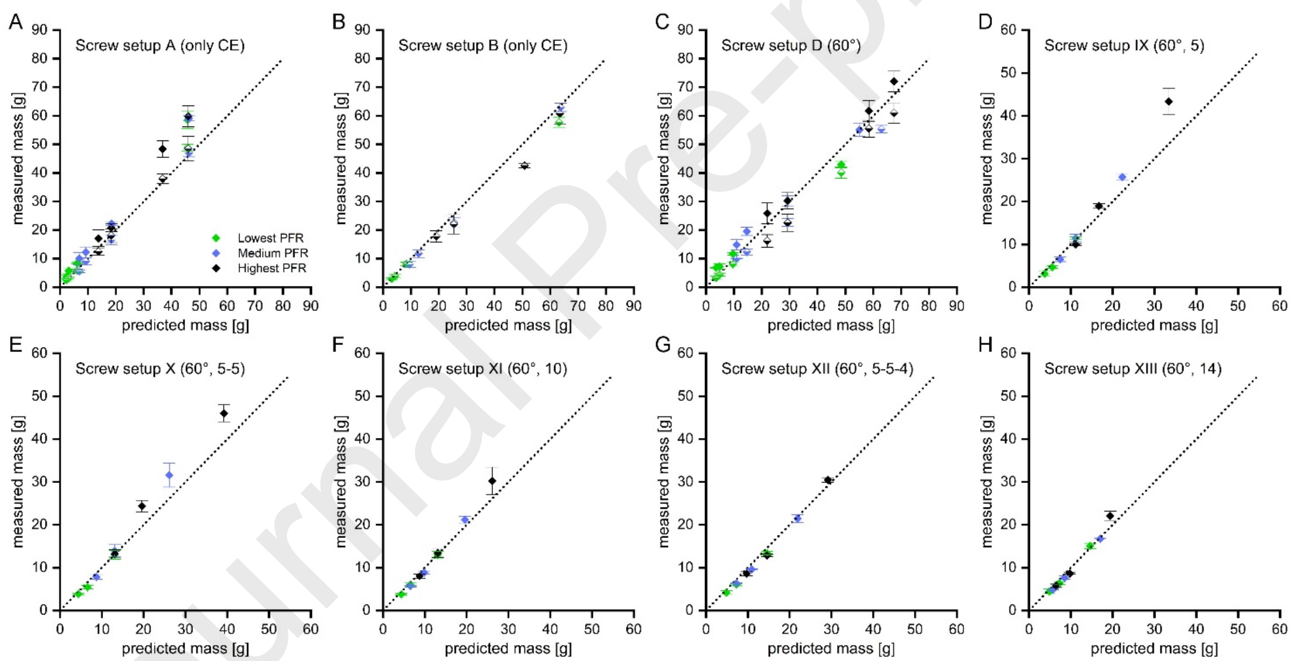

Journal Pre-proofs

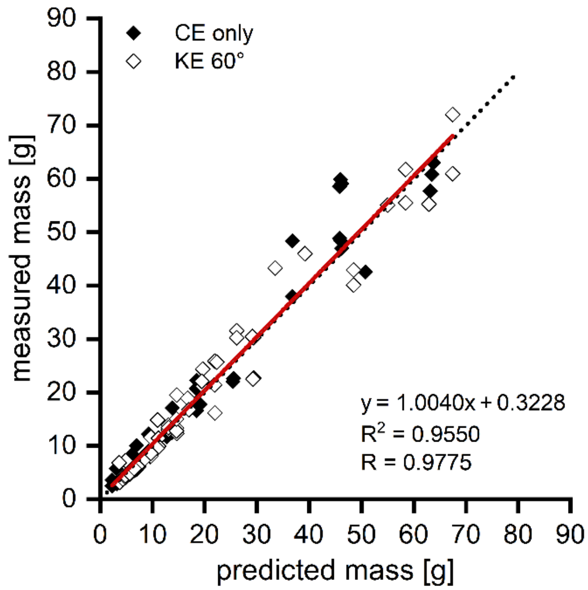

Journal Pre-proofs

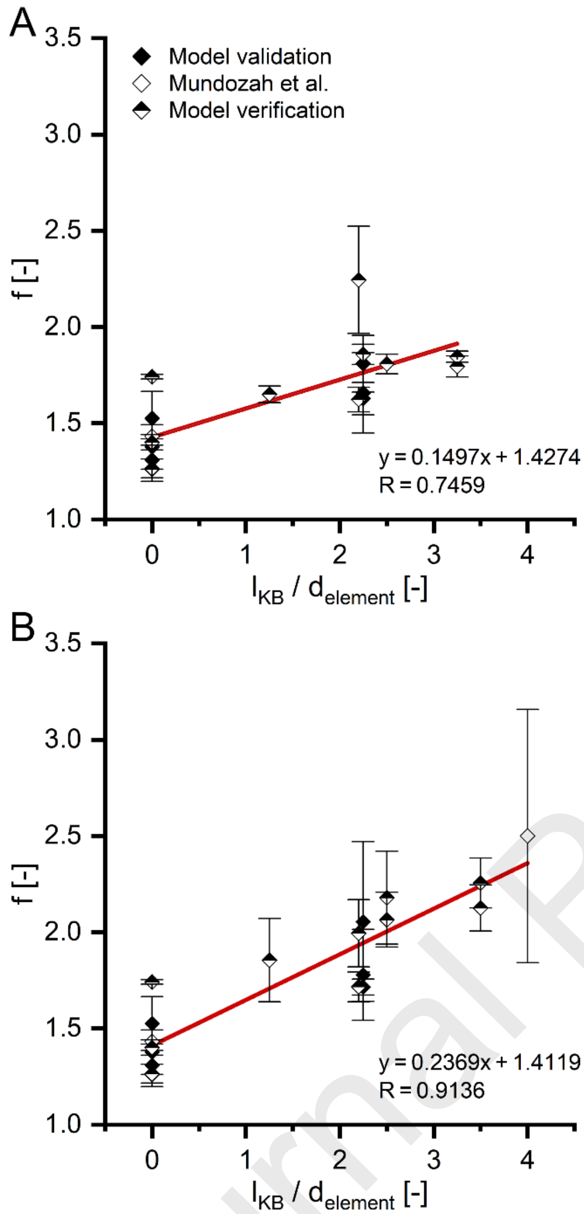

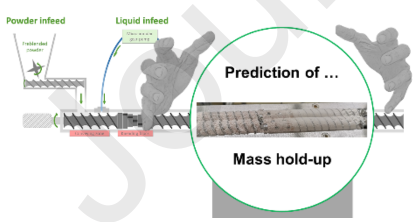

Journal Pre-proofs